

# Simulation Study on ECI for BEPC and its Upgrade Plan BEPCII

J. Xing, Z.Y. Guo, Q. Qin , J.Q. Wang, IHEP

## Abstract

The Beijing Electron Positron Collider (BEPC) will be upgraded to enhance the luminosity in the energy of 1.55 GeV. The machine will become a double ring (BEPCII) from a single ring. The multi-bunch electron and positron beams will circle in each ring respectively. The electron cloud instability is suspected to occur in the positron ring, and it may influence the performance of the collider on the luminosity. A simulation code has been developed based on similar programs, which have been used to study ECI in other laboratories. The physics model of the instability, the simulation results comparing to the observation in the BEPC experiments and simulation results on the BEPCII design study will be discussed in this paper.

# Part I

## Review of Experiment and Simulation study on BEPC

### 1. Instrumentation

#### 1.1 PE detector

Similar to the detector in the APS, a photoelectron detector was installed in the BEPC ring. It has three layers with the same diameter of 80 mm and two mesh grids in front of the detector. The outermost grid is grounded, and a bias voltage is applied to the shielded grid. The graphite-coated collector lowers the secondary electron yield and is biased with a DC voltage of +48 V with batteries. Between the detector and the support barrel mounted on an idle slot, a 1 cm annual gap exists.

Being so close to the dipole, the PE detector has to be shielded from the magnetic field with layers of high and low permeability “mu-metal” sheets and nickel alloy sheets. After shielding, the fields at the points *a* and *b* in Fig. 1 are 9 Gauss and 0, respectively.

## 1.2 Apparatus setup

The detector is connected with other instruments as shown in Fig. 2. A low pass filter (LPF) is used to make sure that the signal of collector is from the electron only. A  $0.1\text{M}\Omega$  resistor checks the direction of the current from the collector, associated with the voltmeter. The current of photoelectron is measured with the nanoammeter, which is connected between the resistor and ground. It can also cross-check the readings of the voltmeter. A temperature monitor is mounted on the detector to detect heat induced by beam-excited HOM wakefields in the annular gap between the detector and the support barrel.

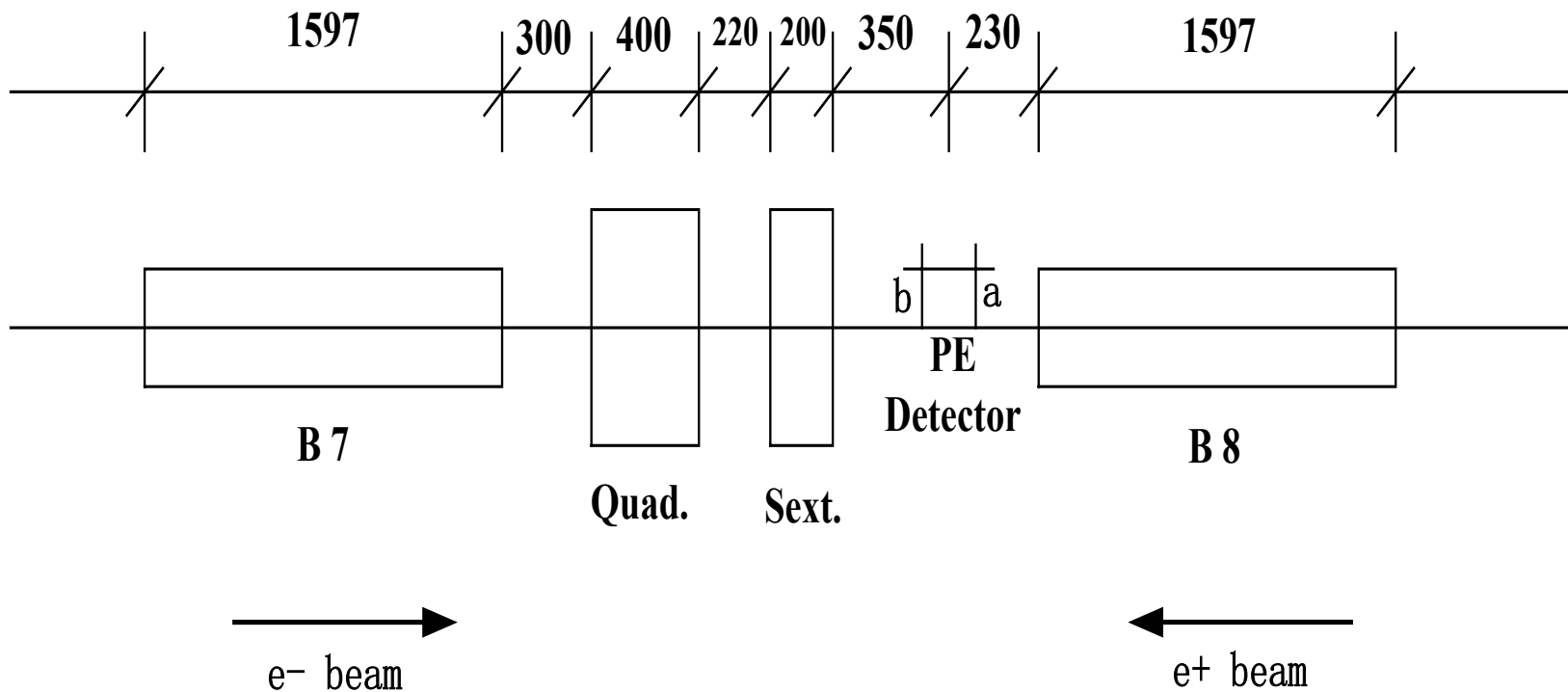


Figure 1: Position of the PE detector at the BEPC storage ring (seen from inside of the ring).

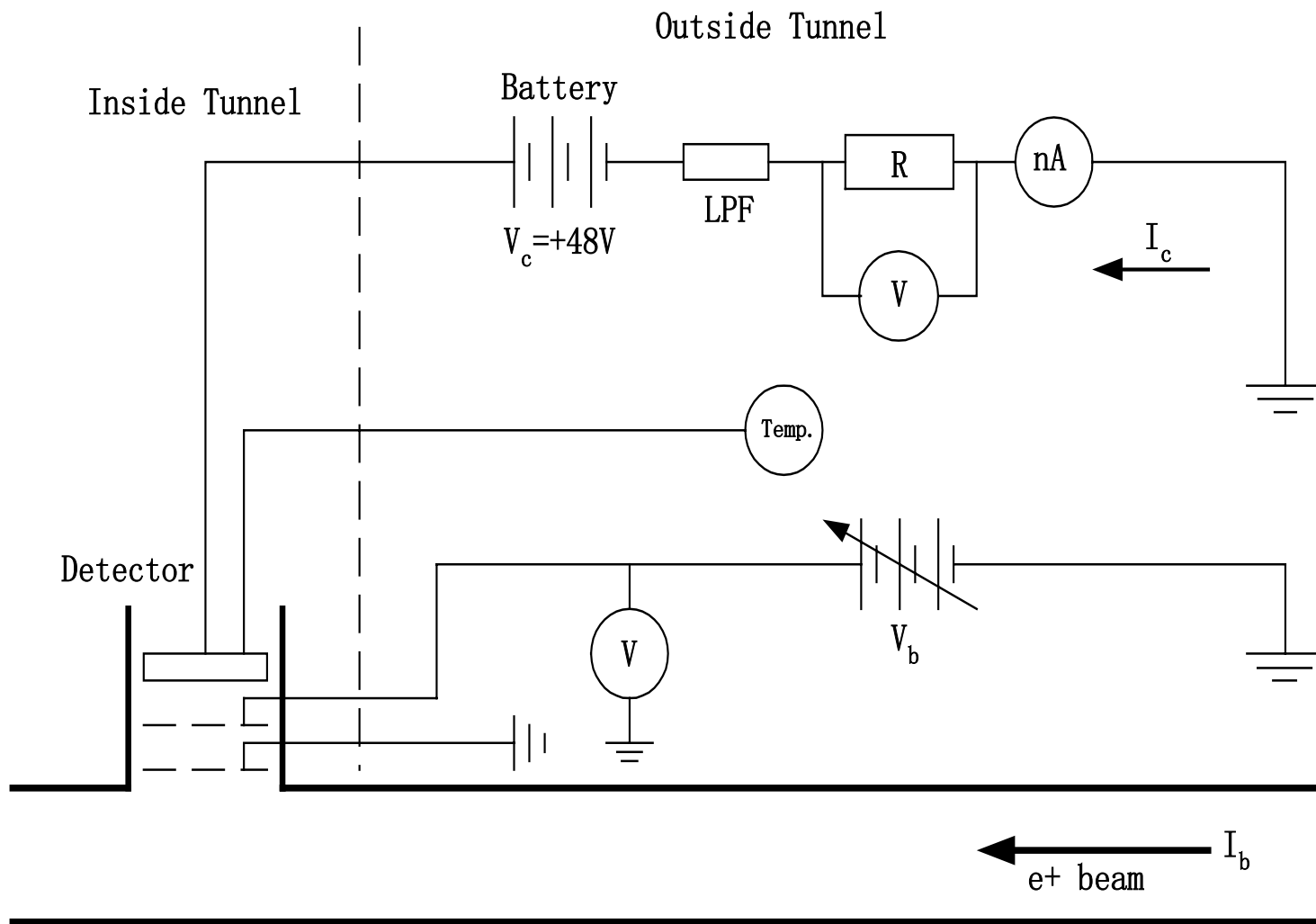


Figure 2: Setup of all apparatus in the experiment.

## 2. Measurements

The LPF filters beam-induced RF noises. In the following PE measurements, we apply the 150 MHz LPF to eliminate any sources of RF noise. During all the measurement, the temperature monitor displays  $24\pm 1^\circ\text{C}$  with no change, which means the HOMs effect due to the annular gap between the detector and its support barrel is minimal. All these confirm the validity of the whole measurement system.

A bias voltage scan was made and the  $V_b$  fixed at +40V for maximum signal, as shown in Fig. 3.

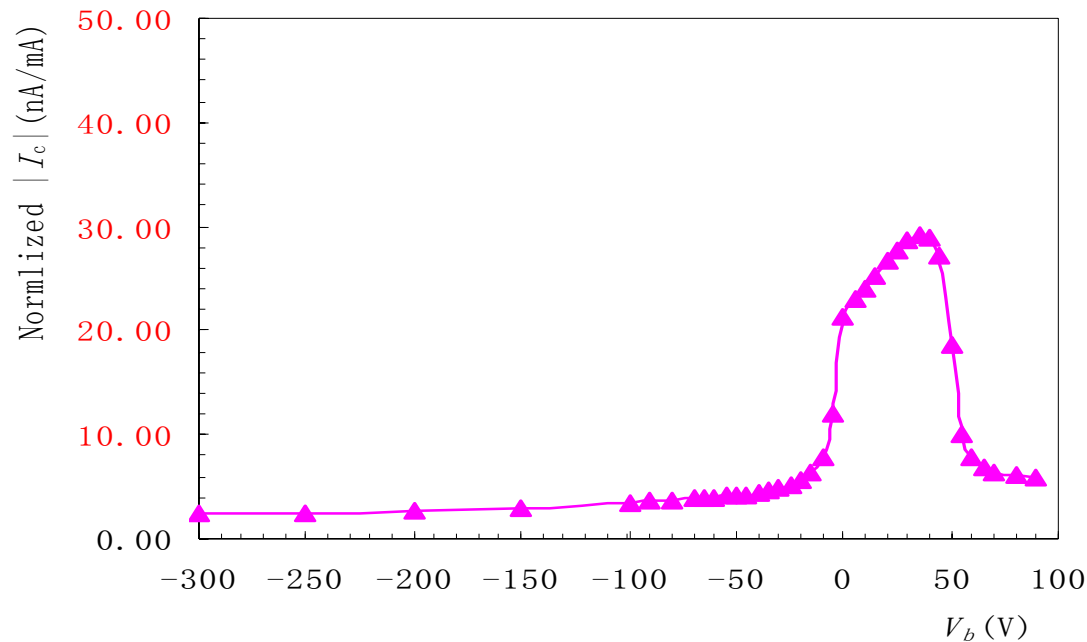


Figure 3: Detector current when bias voltage scans.

The derivative of the normalized  $I_c$ - $V_b$  curve gives the photoelectron energy distribution, shown as Fig. 4.

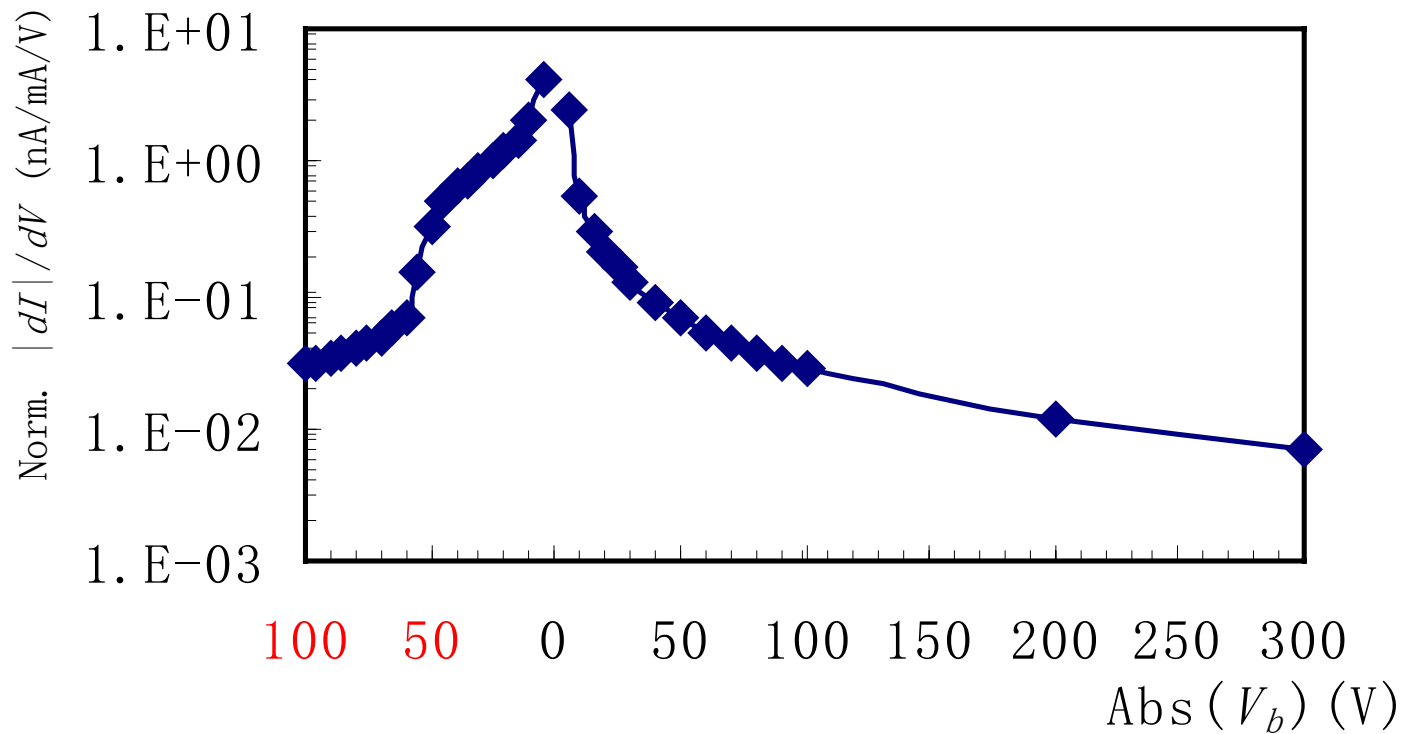


Figure 4: Photoelectron energy distribution.

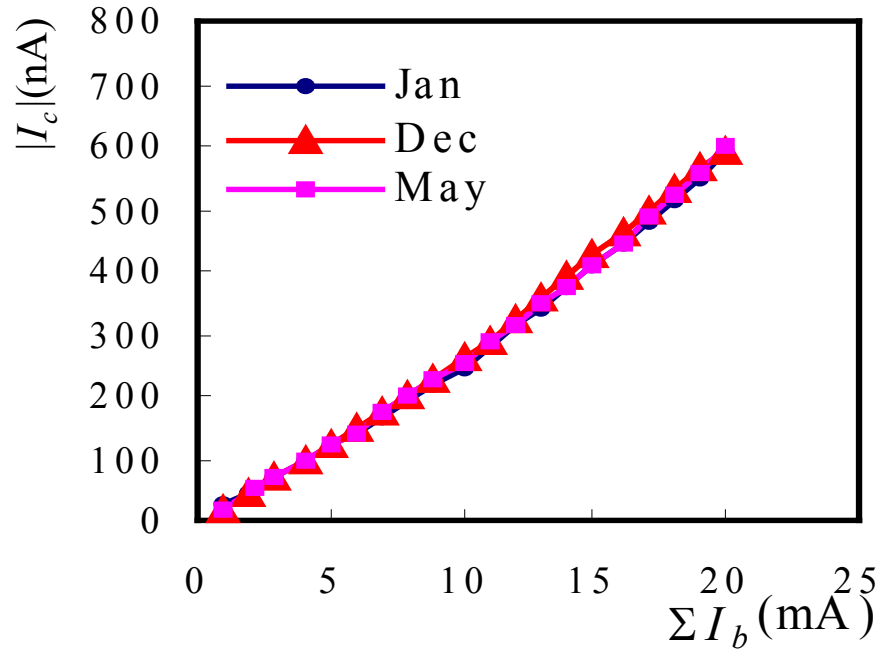


Figure 5: Collected electron current  $I_c$  as a function of beam current  $I_b$

The collected electron current  $I_c$  as a function of beam current  $I_b$  is measured in the cases of single bunch and multi-bunch. Normalized by  $I_b$ ,  $I_c$  is almost the same in different bunch spacing. It reads about 25nA/mA at the bunch current of 2 mA, Fig. 5.

No any saturation effect, in which electron generation and loss equilibrate, is found with a long bunch train and a weak bunch current, even 40 bunches are used with the bunch current of 1 or 2 mA ( $I_b$  is 40 or 80 mA).

### Secondary electron (SE) measurement

Due to the SE, a dramatic amplification of the signal is observed in the APS when the bunch spacing is 7 buckets (20 ns) . But in our measurements, such an amplification is not observed as shown in Fig.6..

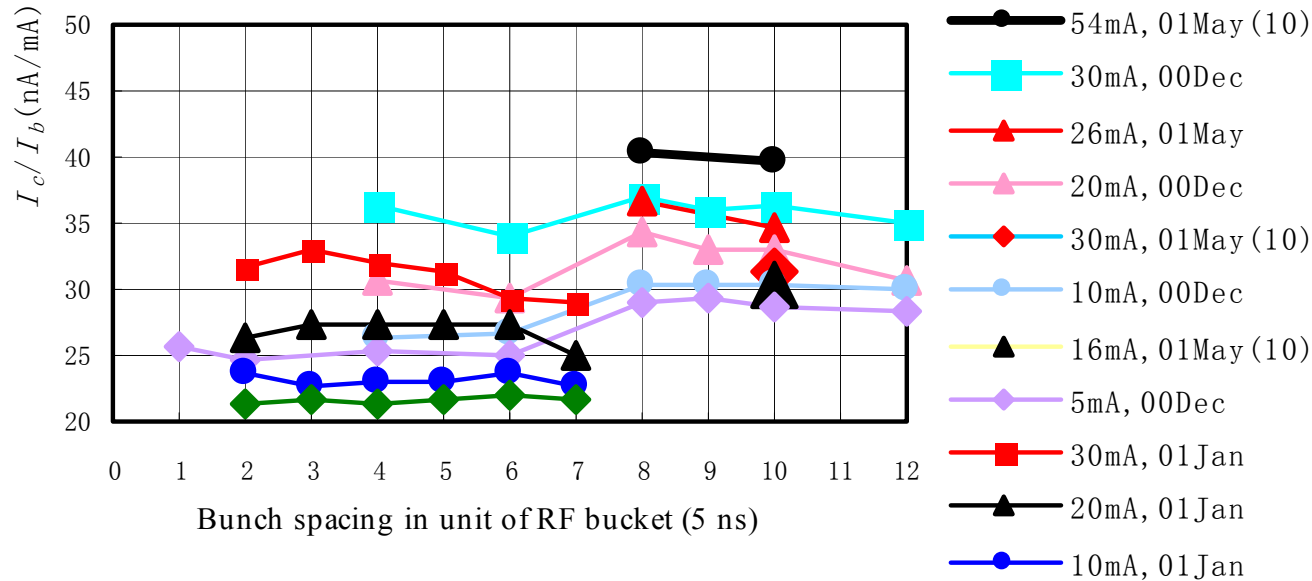


Figure 6: Normalized electron current as a function of bunch spacing and current. The legend gives beam current used.

### ***Solenoid effect***

Solenoid coils winding downstream the dipoles is a possible way to cure the PEI, like KEKB LER. In BEPC storage ring, we installed two coils on each side of the detector to observe the solenoid effect. The currents of the coils,  $I_s$ , are  $\pm 20\text{A}$ , generating several tens of Gauss magnetic field. Fig. 7 shows the  $I_c$  vs.  $I_b$  when solenoid has different currents.

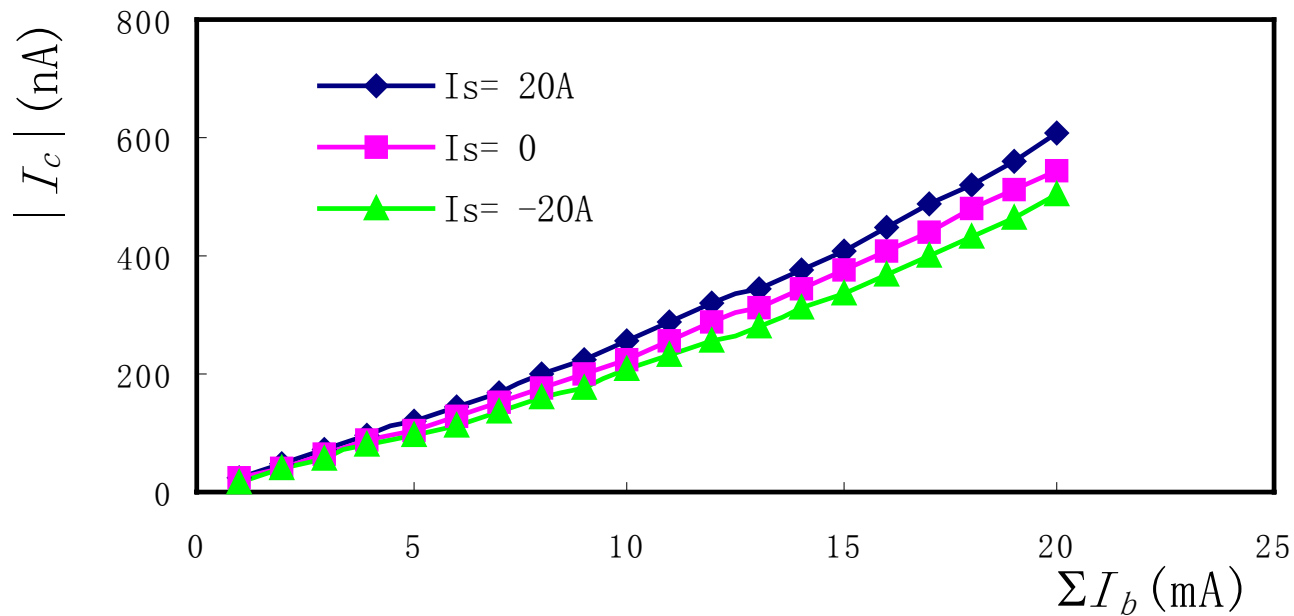


Figure 7:  $I_c$  vs.  $I_b$  with different solenoid fields.

### 3. Simulations

With the code developed by Dr. Y. Luo , the PE generation is simulated for different PE reflectivity. For a real machine, a reflectivity of 0.98 is chosen in simulation. The energy distribution of the PE is selected as  $5\text{eV}\pm 5\text{eV}$ . The emission yield of secondary electron is given as with  $\cos\theta$  distribution as the angle distribution. The energy distribution of the SE is  $0\pm 5\text{eV}$ , and the  $\delta_{max}$  of the SE is 3 in simulation.

Table 1: Parameters of BEPC

Energy[GeV]	1.3	Chamble half width[mm]	60
Circumference[m]	240	Chamble half height[mm]	30
Tunes( $Q_x, Q_y$ )	5.82, 6.86	Rms bunch length[mm]	25
Synchrotron tune	0.022	Rms hor. beam size[mm]	1.2
Rms energy spread	$4.1\times 10^{-4}$	Rms vert. beam size[mm]	0.2
Mom. compaction factor	0.04	Bunch space[m]	1.5

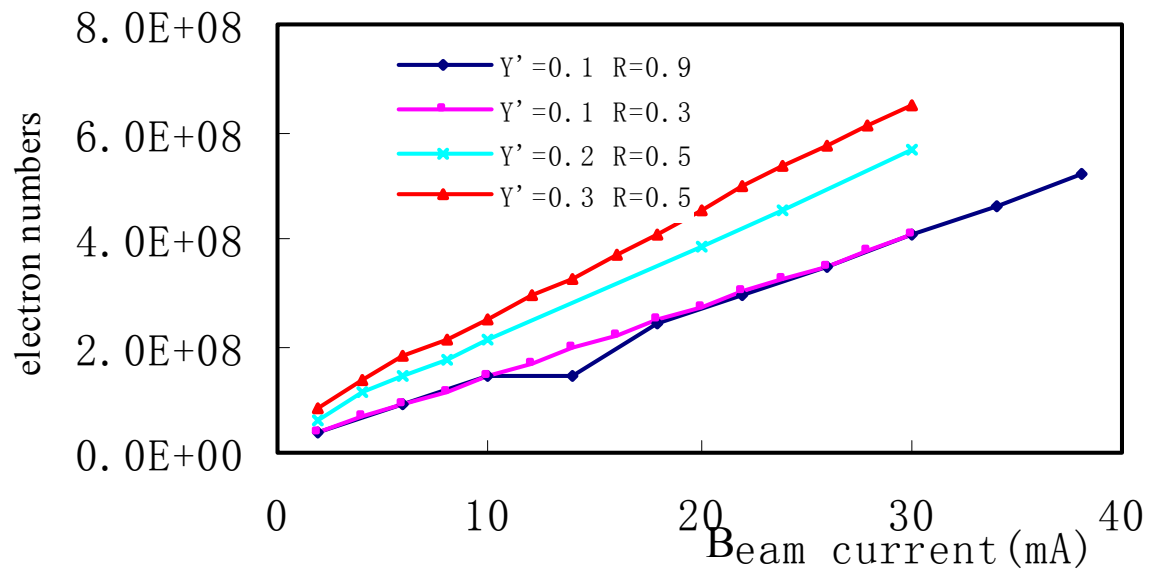


Figure 8: PE creation for different yield and reflectivity.

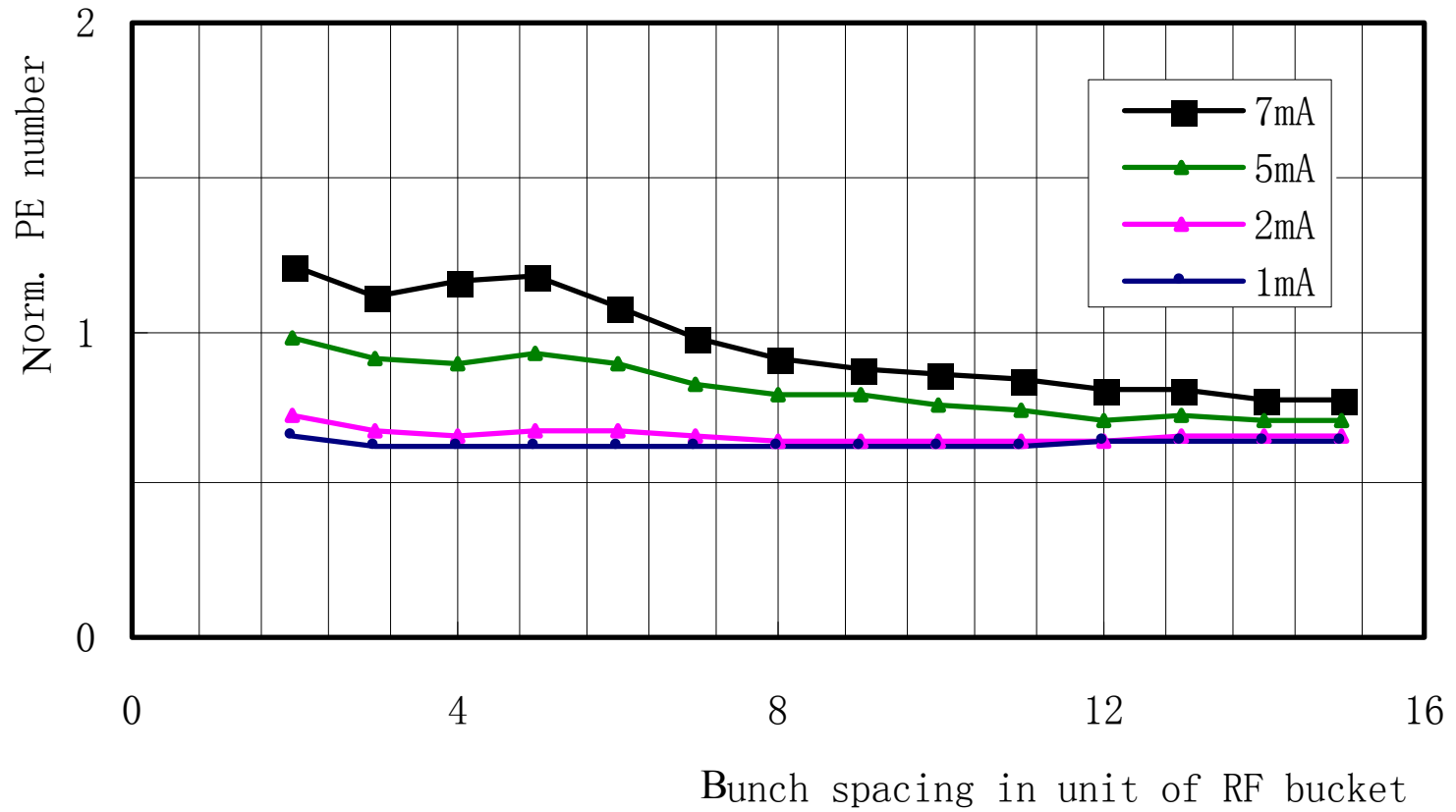


Figure9: Simulation results on multipacting. ( The legend gives bunch current.)

## Part II Simulation study on BEPCII

BEPCII is an upgrade project of Beijing electron-positron collider(BEPC), which will install a new inner ring based on the single-ring collider BEPC. It will provide the colliding beams of the center-mass between  $1.0 \text{ GeV} \times 2$  and  $2.0 \text{ GeV} \times 2$  and also the dedicated synchrotron radiation beam at  $2.5 \text{ GeV}$ . For the colliding beams the luminosity is optimized at  $1.89 \text{ GeV}$  with  $1 \times 10^{33} \text{ cm}^{-2}\text{s}^{-1}$ , which is two order of magnitude of BEPC.

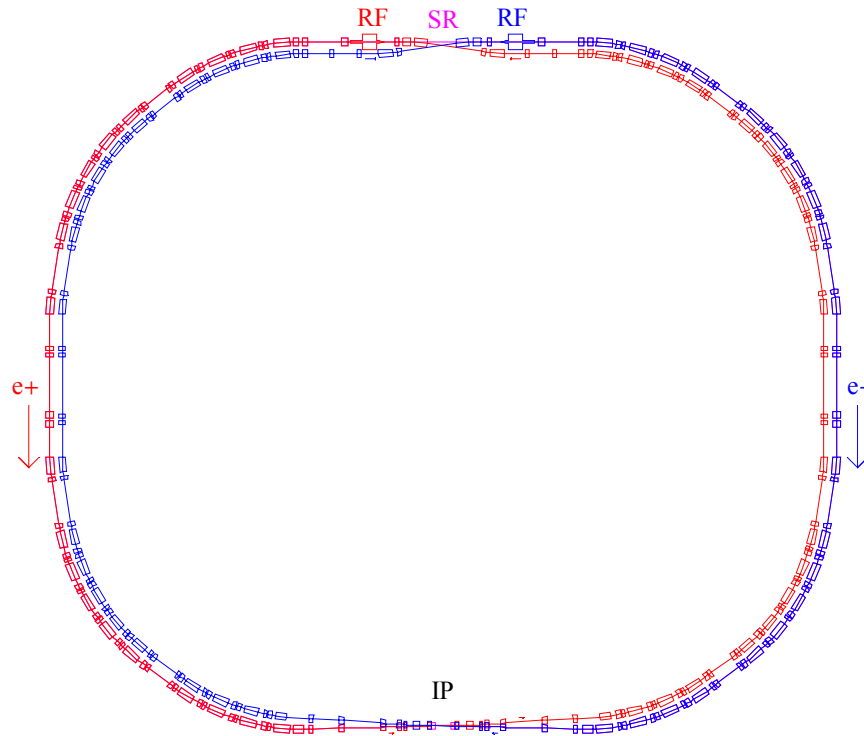


Figure.10 Schematic layout of BEPCII

Table 2: Main parameters of BEPCII

Beam energy $E$	GeV	1.89
Circumference $C$	m	237.53
Harmonic number $h$		396
RF frequency $f_{rf}$	MHz	499.8
RF voltage $V_{rf}$	MV	1.5
Synchrotron radiation loss/turn $U_0$	keV	121
Damping time $\tau_x/\tau_y/\tau_E$	ms	25/25/12.5
Number of particles $N$		$4.510^{12}$
Natural energy spread $\sigma_\delta$		$5.1610^{-4}$
Momentum compact $\alpha_p$		0.0235
Bunch length $\sigma_z$	cm	1.5
Emittance $\varepsilon_x/\varepsilon_y$	nm-rad	144/2.2
$\beta$ function at IP	m	1/0.015
Betatron tune $\nu_x/\nu_y/\nu_s$		6.57/7.61/0.034
Natural chromaticities $\nu_x'/\nu_y'$		-11.9/-25.4
Crossing angle at IP $\phi_c$	mrad	11.2
Piwinski angle $\Phi$	rad	0.435
Bunch spacing $s_b$	m	2.4
Beam-beam parameters $\xi_x/\xi_y$		0.04/0.04
Luminosity $\mathcal{L}$	$\text{cm}^{-2}\text{s}^{-1}$	$1.010^{33}$

Table 3: Parameters of a few storage rings

	BEPCII	KEKB	PEPII
Beam energy(GeV)	1.89	3.5	3.1
Bunch population $N_b(10^{10})$	4.84	3.3	9
Bunch spacing $L_{sep}(m)$	2.4	2.4	2.5
Rms bunch length $\sigma_z(m)$	0.015	0.004	0.013
Rms bunch sizes $\sigma_{x,y}(mm)$	1.18,0.15	0.42,0.06	1.4,0.2
Chamber half dimensions $h_{x,y}(mm)$	60,27	47	25
Slippage factor $\eta (10^{-3})$	22	0.18	1.3
Synchrotron tune $Q_s$	0.033	0.015	0.03
Circumference C(km)	0.24	3.0	2.2
Average beta function(m)	10	15	18
<b>Parameter <math>n_{min}</math></b>	9.24	10	1
<b><math>e^-</math> oscillation/bunch <math>n_{osc} \equiv \omega_e \sigma_z / (\pi c)</math></b>	0.42	1.0	0.9
<b>Density enhancement <math>H_e</math></b>	15	13	12
<b>Adiabaticity A</b>	17.4	9	8
<b>TMCI threshold <math>\rho_e [10^{12}m^{-3}]</math></b>	22.7	0.5	1
<b>Density ratio <math>\rho_{e,sat} / \rho_{e,threshold}</math></b>	0.19	4	4

# 1. Build up and Saturation

The E-CLOUD programme developed by O. BRUNING, G. RUMOLO, F. ZIMMERMANN of the CERN SL Division was used in the simulation study on the build up and saturation of the electron cloud on BEPCII.

Table 4: Parameters used in simulation

Energy[GeV]	1.89	Bunch population[mm]	$4.8 \times 10^{10}$
Circumference[m]	240	Rms bunch length[mm]	15
Chamble radius[mm]	42	Rms hor. beam size $\sigma_x, \sigma_y$ [mm]	2,0.3
Tunes( $Q_x, Q_y$ )	6.6, 7.6	Photonelectron yield $Y_{pe}$	0.006
Synchrotron tune	0.033	Photon reflectivity $R$	100%
Rms energy spread	$5.16 \times 10^{-4}$	Center of photonelectron energy distr. $E_{pe,0}$ (eV)	5
Mom. compaction factor	0.02	Photonelectron rms energy spread $\sigma_{pe}$ (eV)	5
Shunt-impedance[M $\Omega$ /m]	0.066	Maximum secondary emission yield $\delta_{max}$ (SEY)	1.066
Bunch space[m]	2.4	Energy of max. sec. emission $\epsilon_{max}$ (eV)	350

## Effect of the photo-emission yield and the SEY

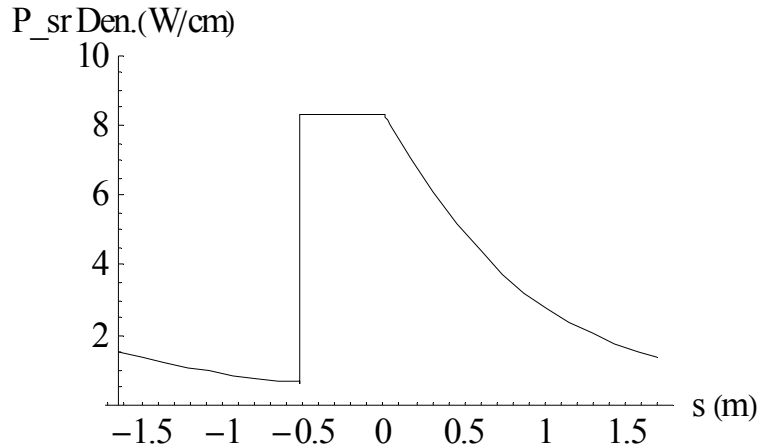


Figure11: SR power distribution along the ring  
 (-1.6 < s < 0, means in the dipole magnet region,  
 0 < s < 1.7, means in the free field region )

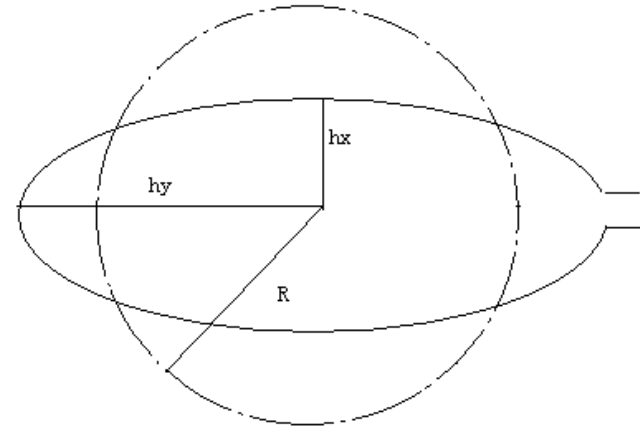


Figure12: circle chamber used in simulation vs.  
 design elliptic chamber with antichamber  
 (R = 42mm, hx = 27mm, hy = 60mm)

The number of radiated photons per positron is given by 
$$N_{\gamma/p} = \frac{5 \alpha \gamma}{2 \sqrt{3}} \Delta \theta$$

For BEPCII, it means about **12** photons for one dipole bending magnet. From figure 10. , the “first strike” photons in the dipole magnet region is approximately **equal** to that in the field free region. And consider the effect of the antichamber, only **~1%** of the radiated photons can remain inside the chamber. Assume the electron yield per absorbed photon is 0.1, then the photonelectron yield  $Y_{pe}$  will be 0.006.

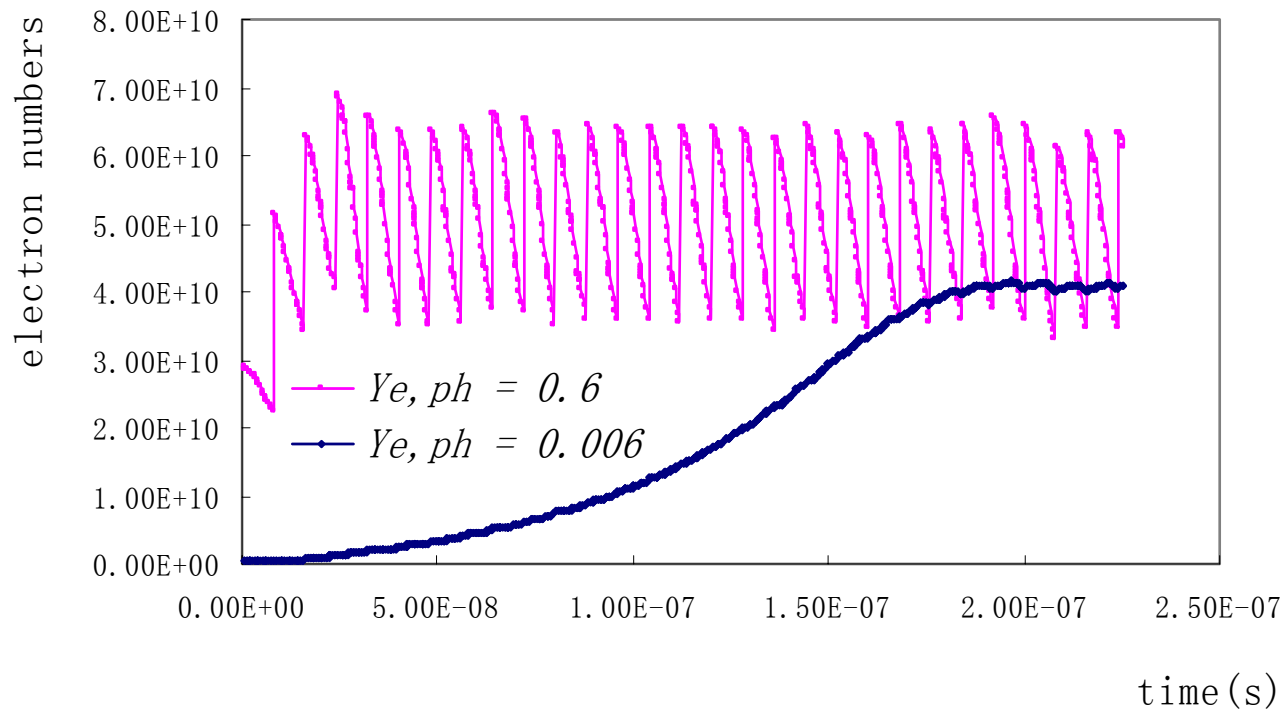


Figure13: Electron numbers with and. without antichamber. ( $\delta_{\max}=3$ )

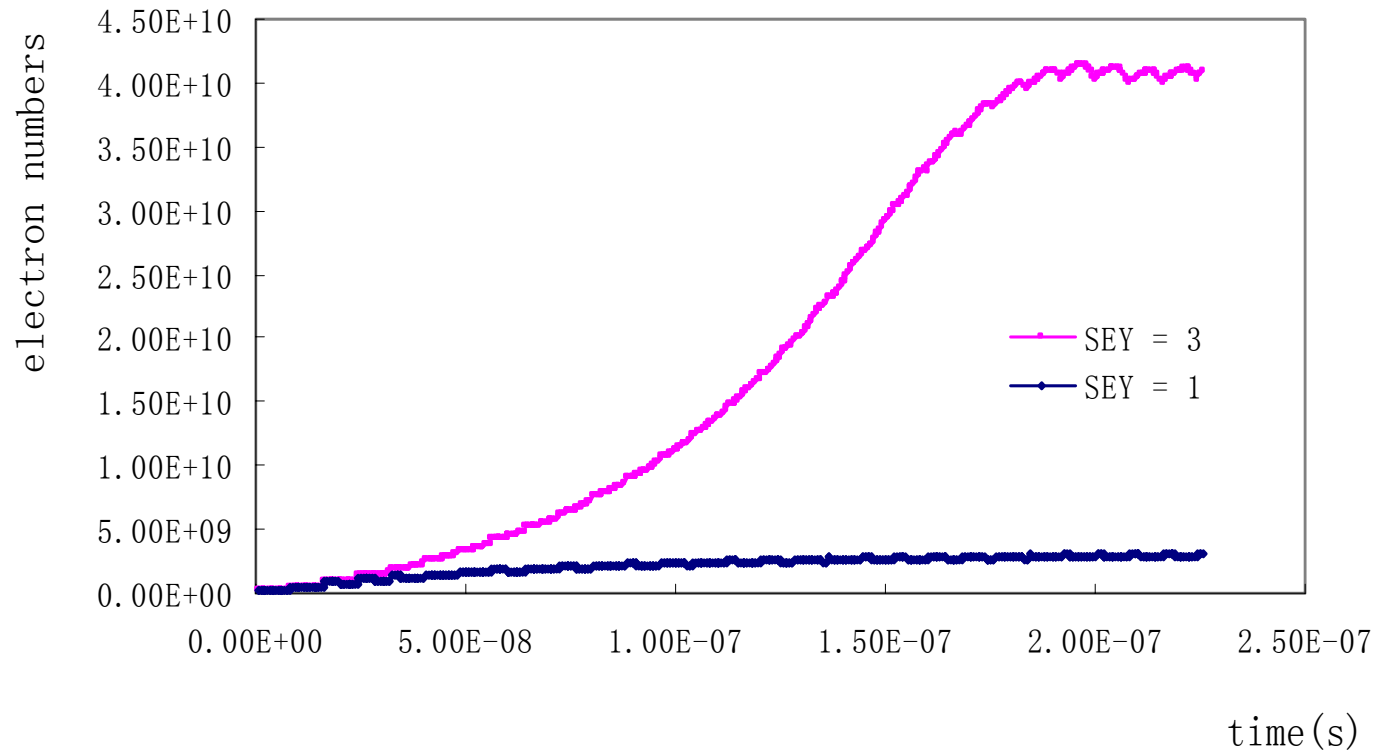


Figure14: Electron numbers with and. without TiN coated of the chamber. ( $Y_{e,ph}=0.006$ )

## Field- free region

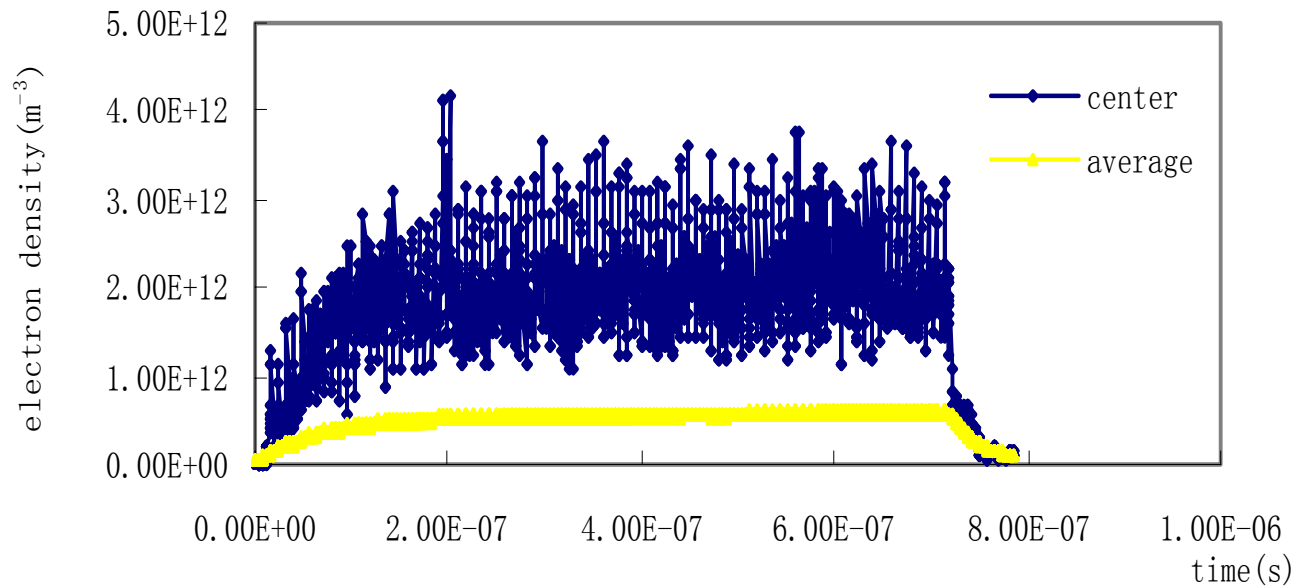


Figure 15: Electron density at the pipe center and the average density of the pipe per cubic meter for a field-free region vs. time in seconds.

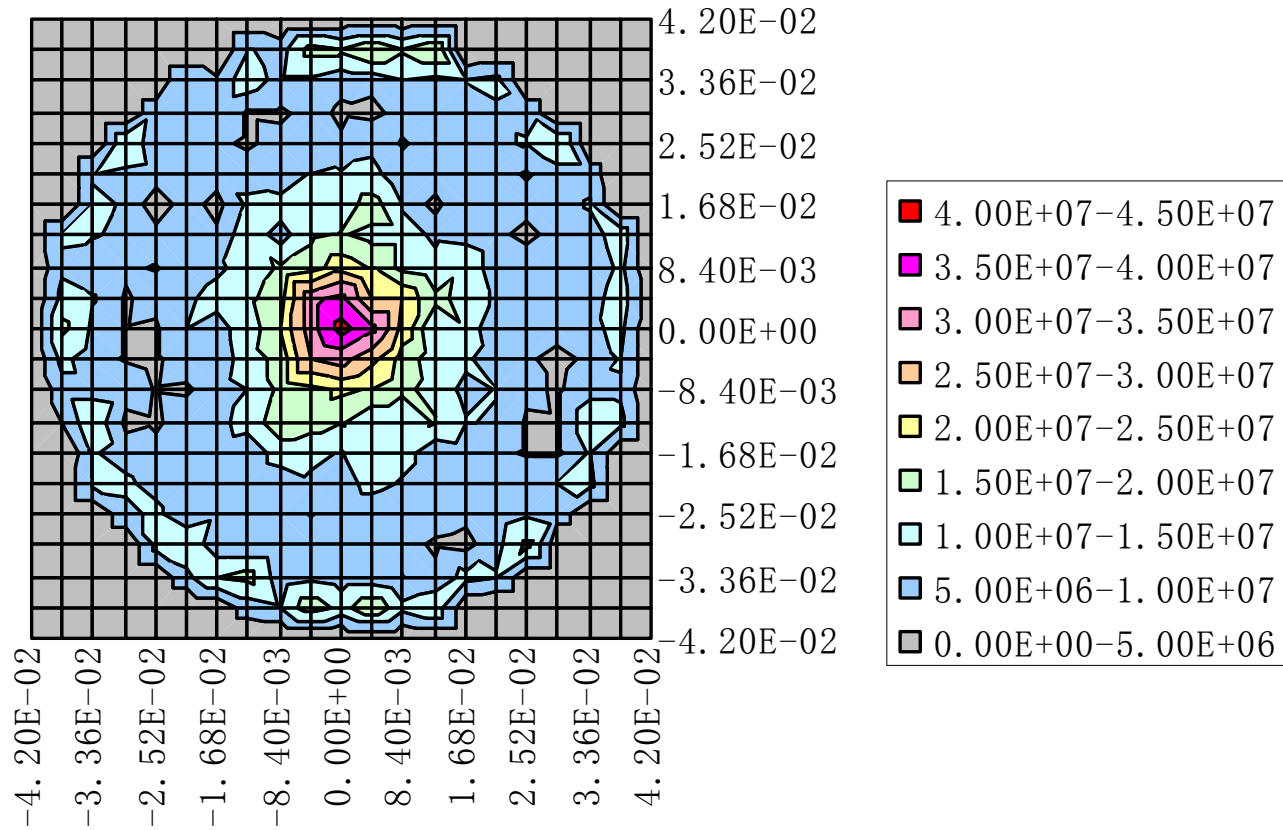


Figure 16: Ecloud transvers distribution after a bunch passed in the free field region.

## Dipole bending magnet

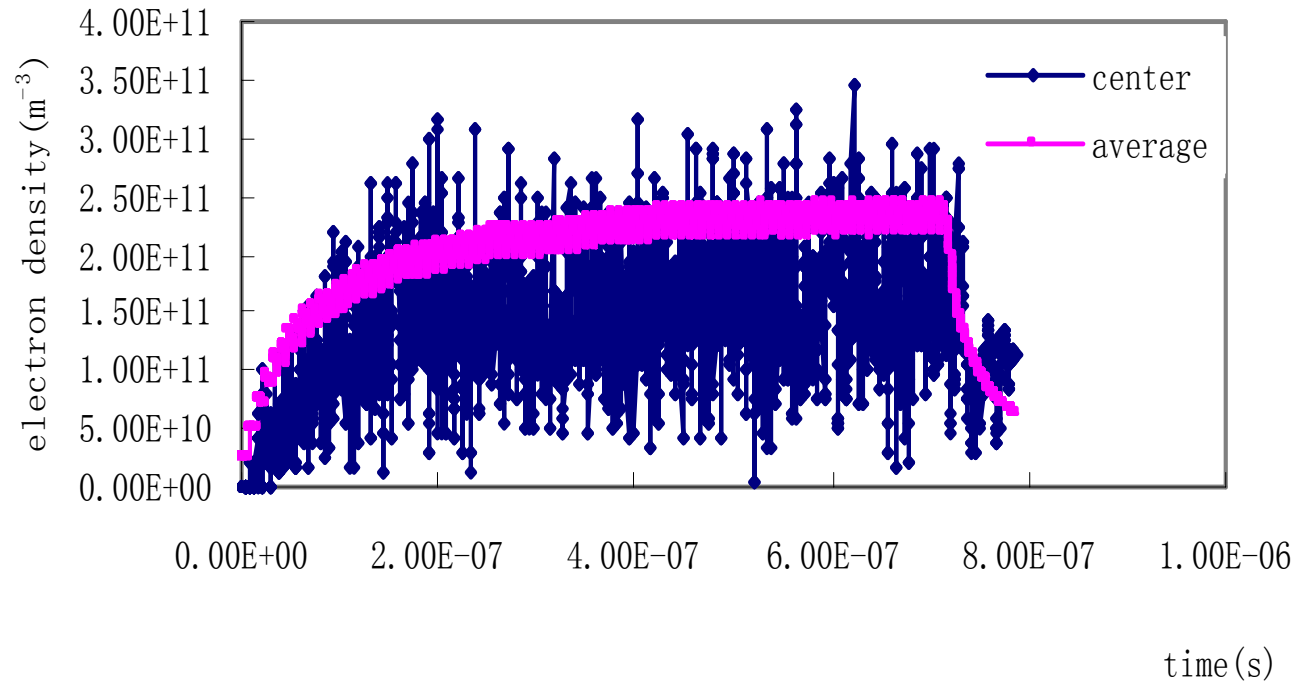


Figure 17: Electron density at the pipe center and the average density of the pipe per cubic meter for a dipole bending magnet region vs. time in seconds.

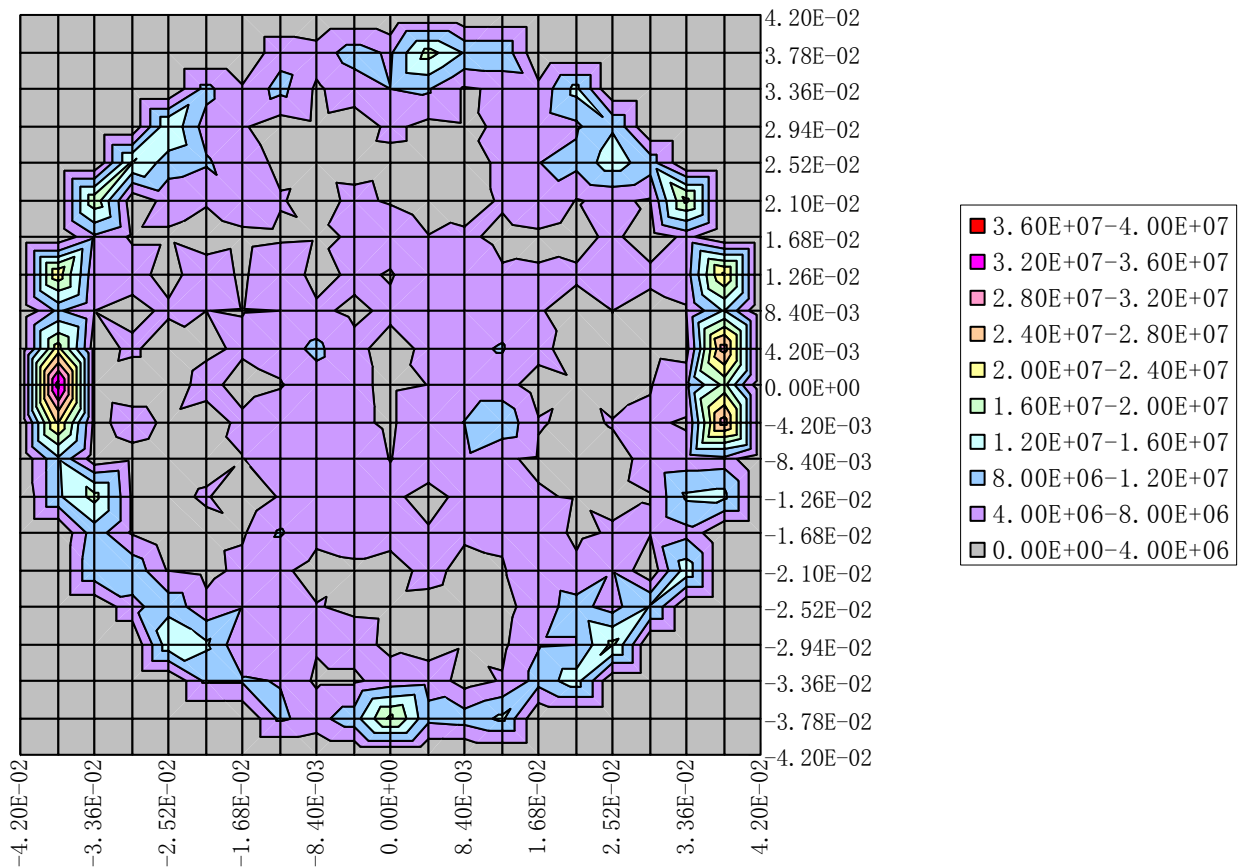


Figure 18: Ecloud transversal distribution in the dipole magnet.

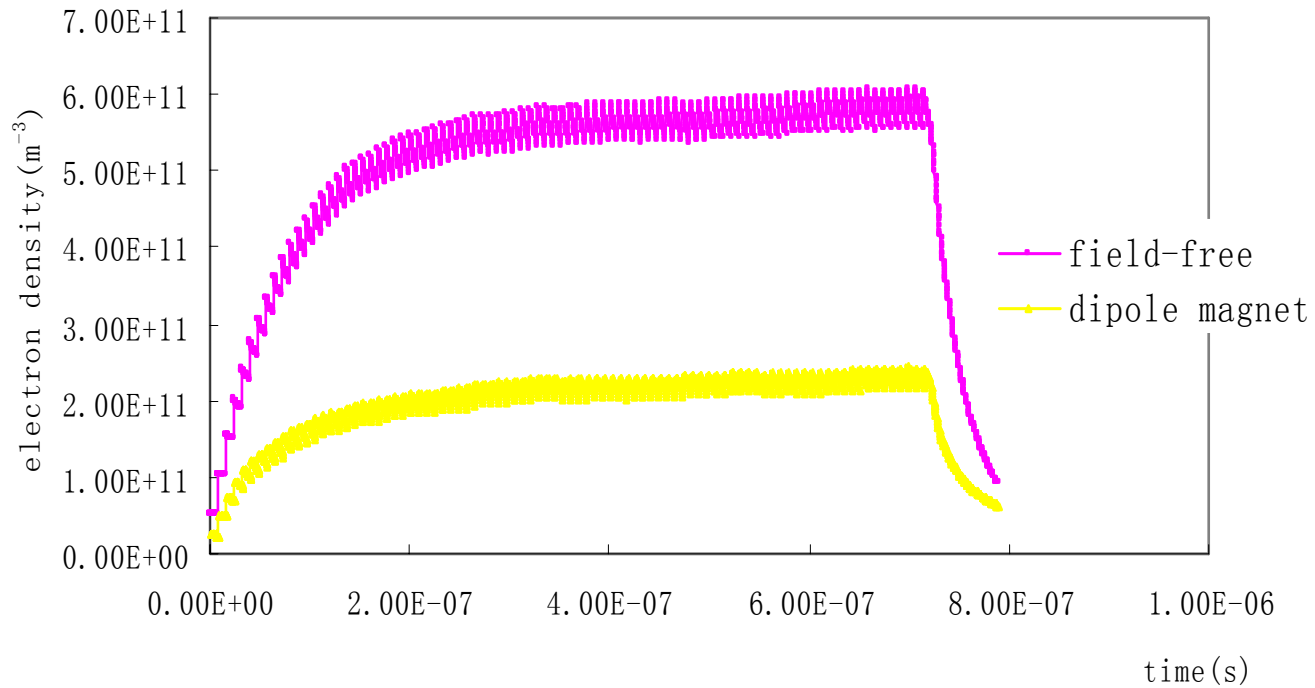


Figure 19: the average electron density of the pipe per cubic meter in the free field region compared with that in the dipole magnet.

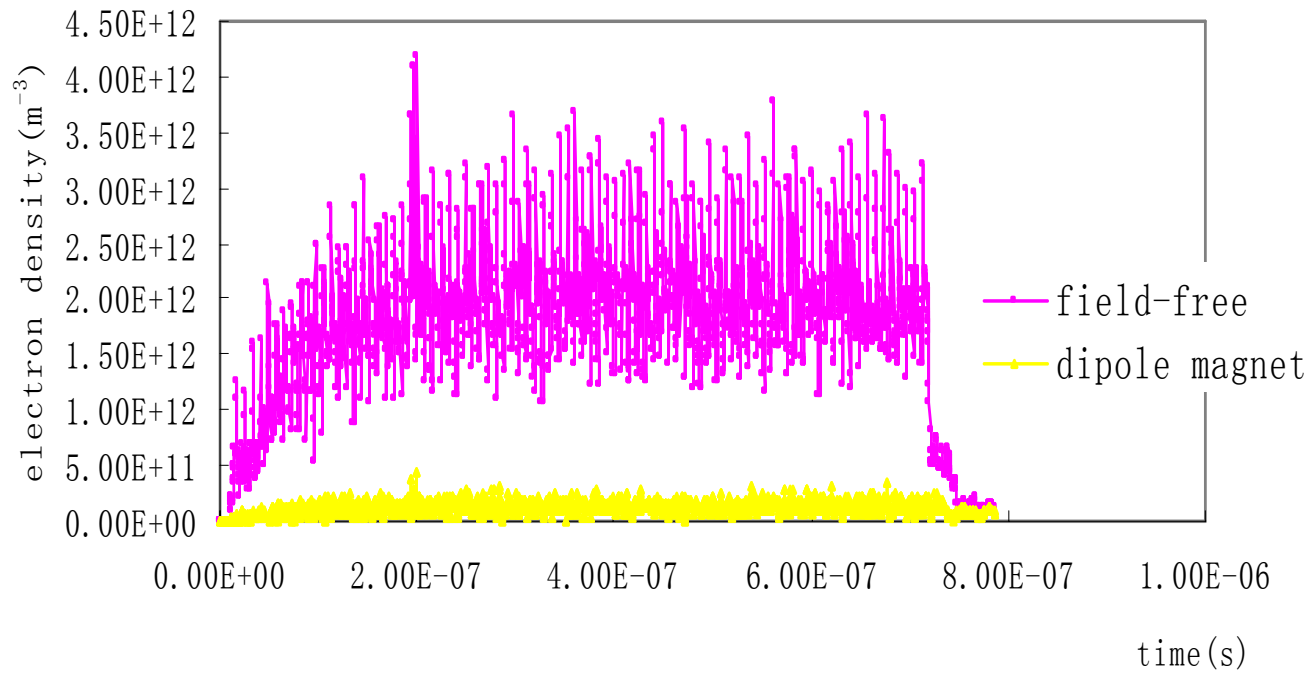


Figure 20: Electron density at the center of the pipe per cubic meter in the free field region compared with that in the dipole magnet.

## Drift space with solenoid

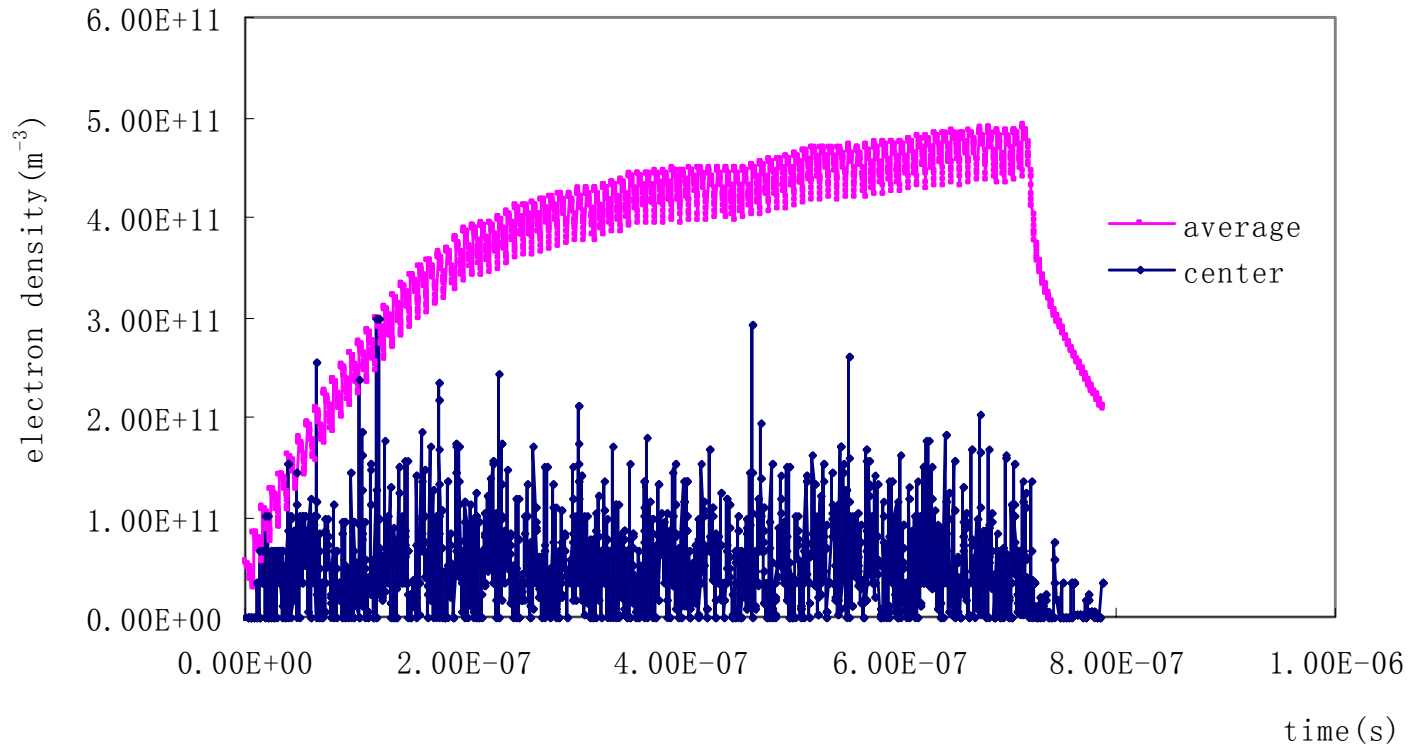


Figure 21: Electron density at the pipe center and the average density of the pipe per cubic meter for a field-free region with solenoid( $B_z=30\text{Gauss}$ ) vs. time in seconds.

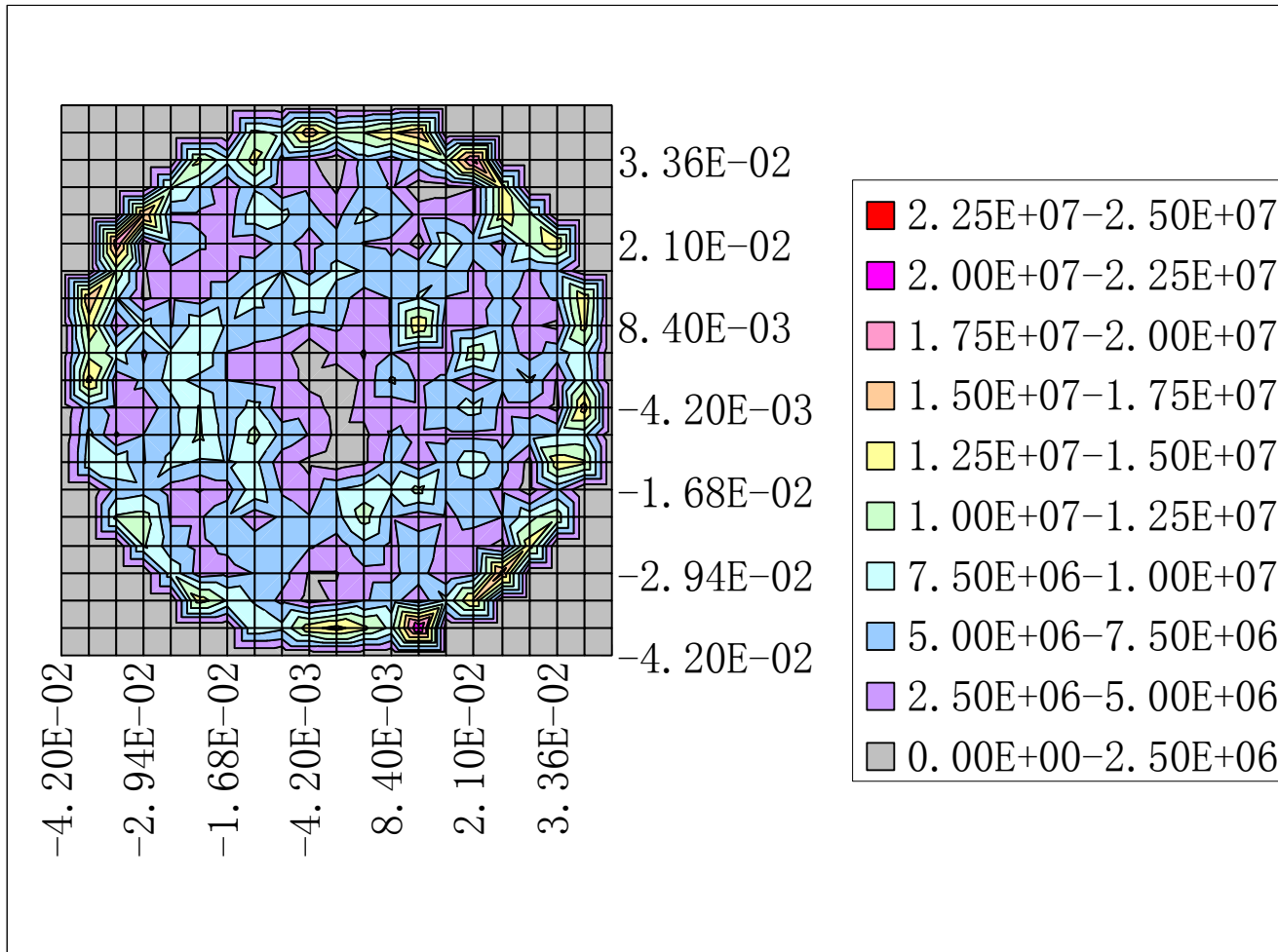


Figure 22: Ecloud transversal distribution in the free field region with solinoid.

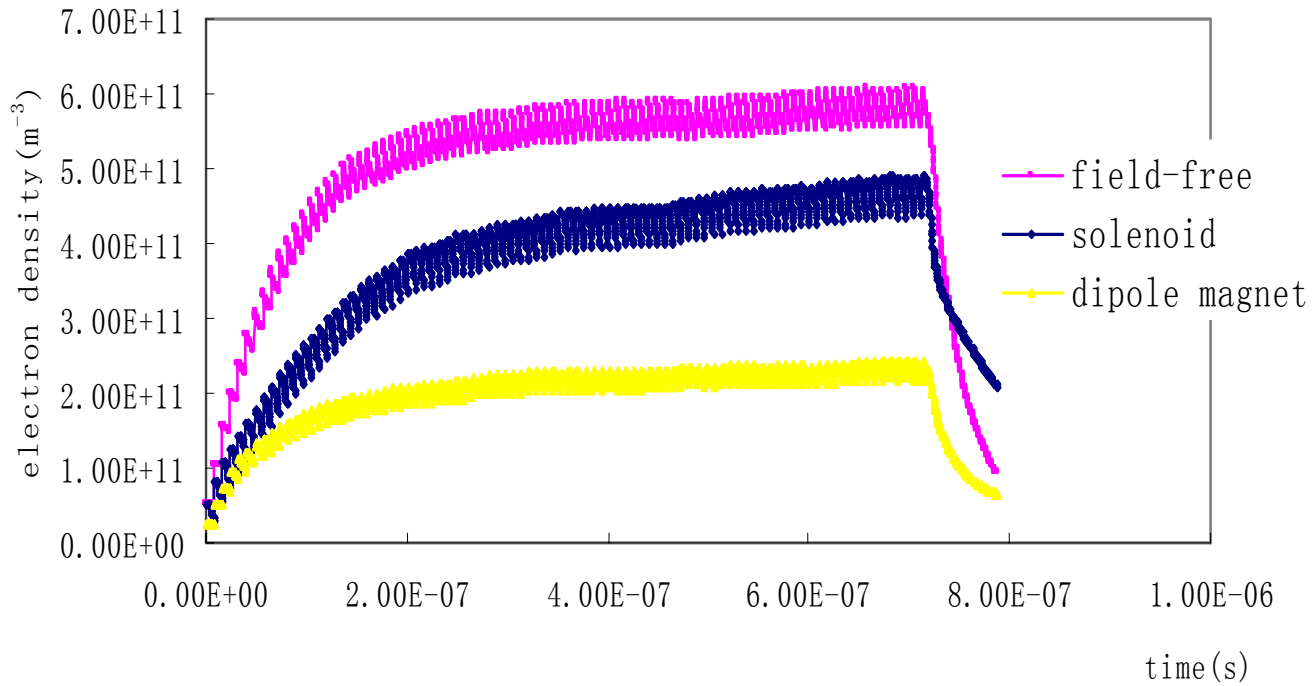


Figure 23: the average electron density of the pipe per cubic meter in the dipole magnet compared with that in the free field region with and without solenoid.

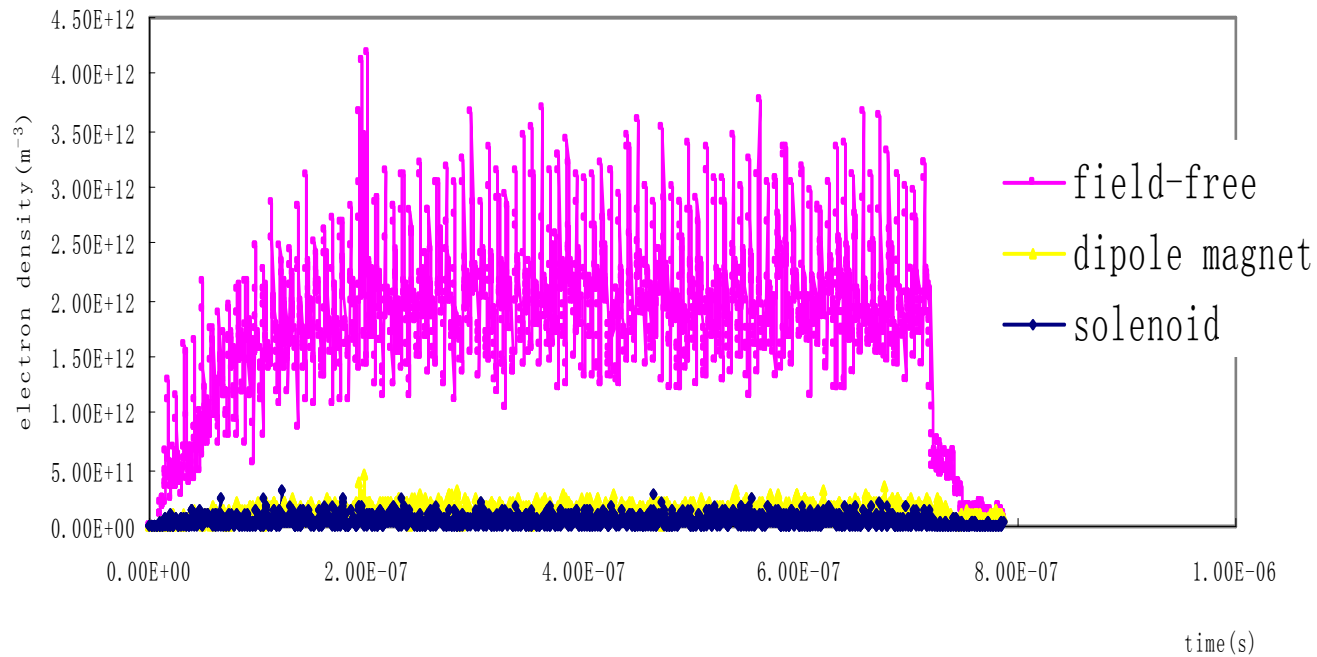


Figure 24: Electron density at the center of the pipe per cubic meter in the dipole magnet compared with that in the free field region with and without solenoid.

## Effect of the clearing electrode

### field-free region

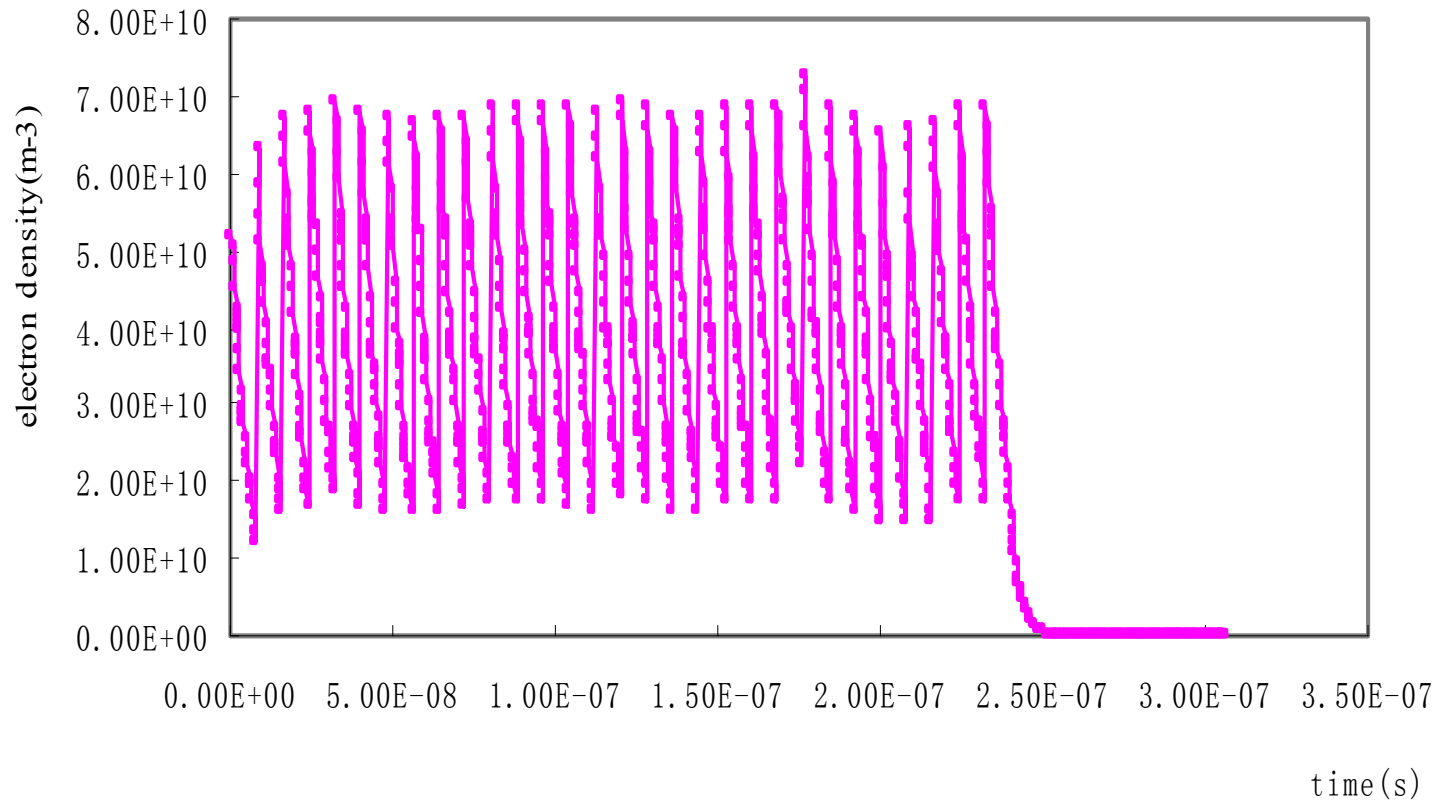


Figure 25: the average electron density of the pipe per cubic meter for a field-free region with clearing electrode (250V) vs. time.

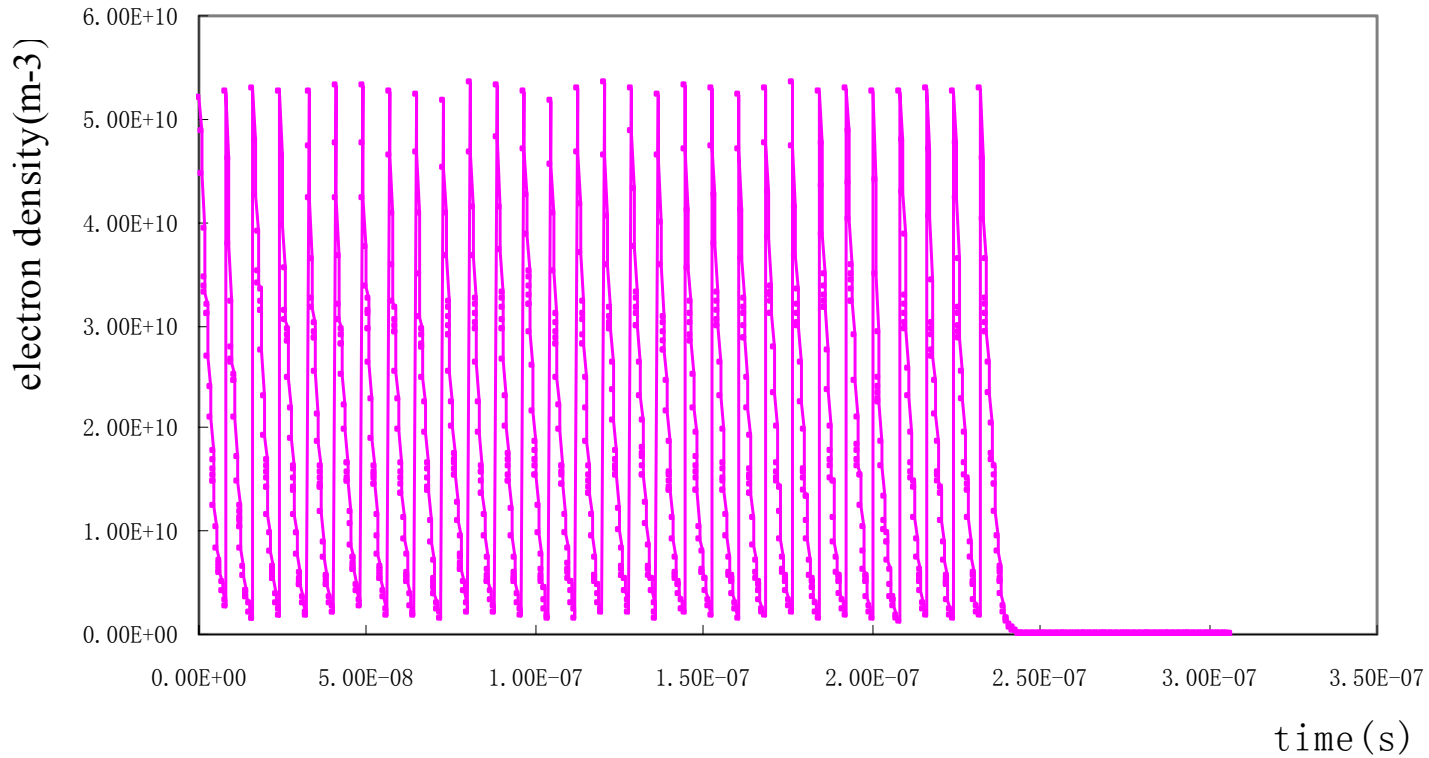


Figure 26: the average electron density of the pipe per cubic meter for a field-free region with clearing electrode (500V) vs. time.

## Dipole magnet region

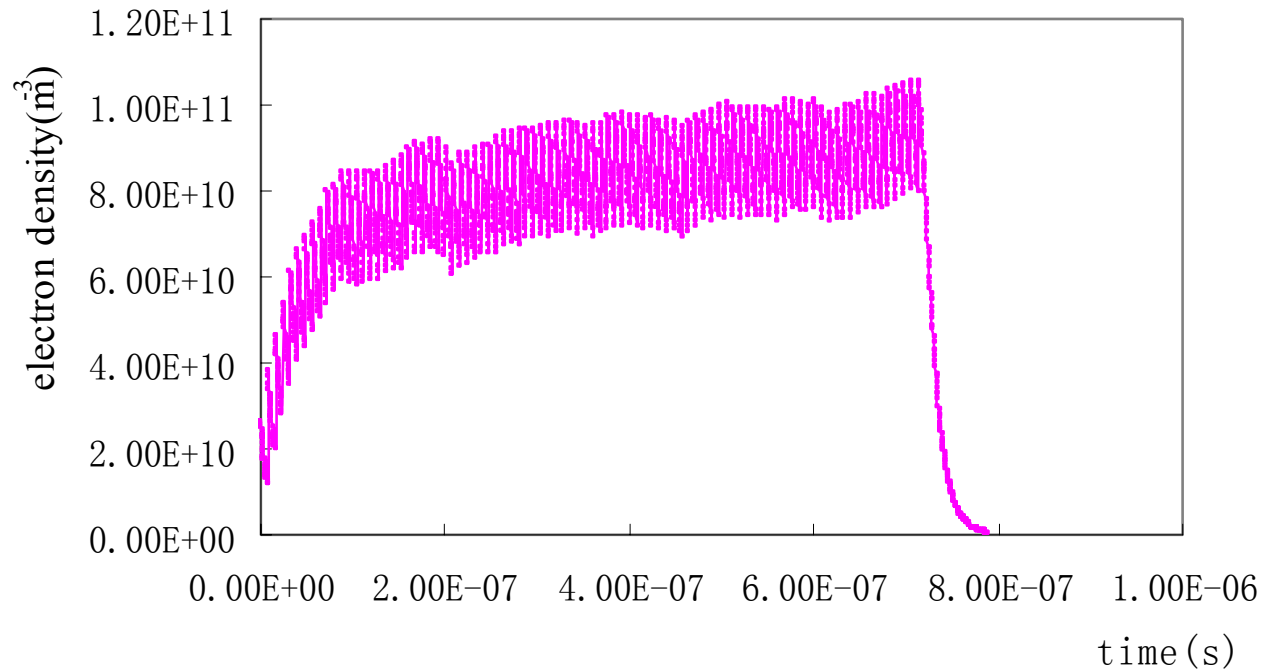


Figure 27: the average electron density of the pipe per cubic meter for a dipole magnet region with clearing electrode (500V) vs. time.

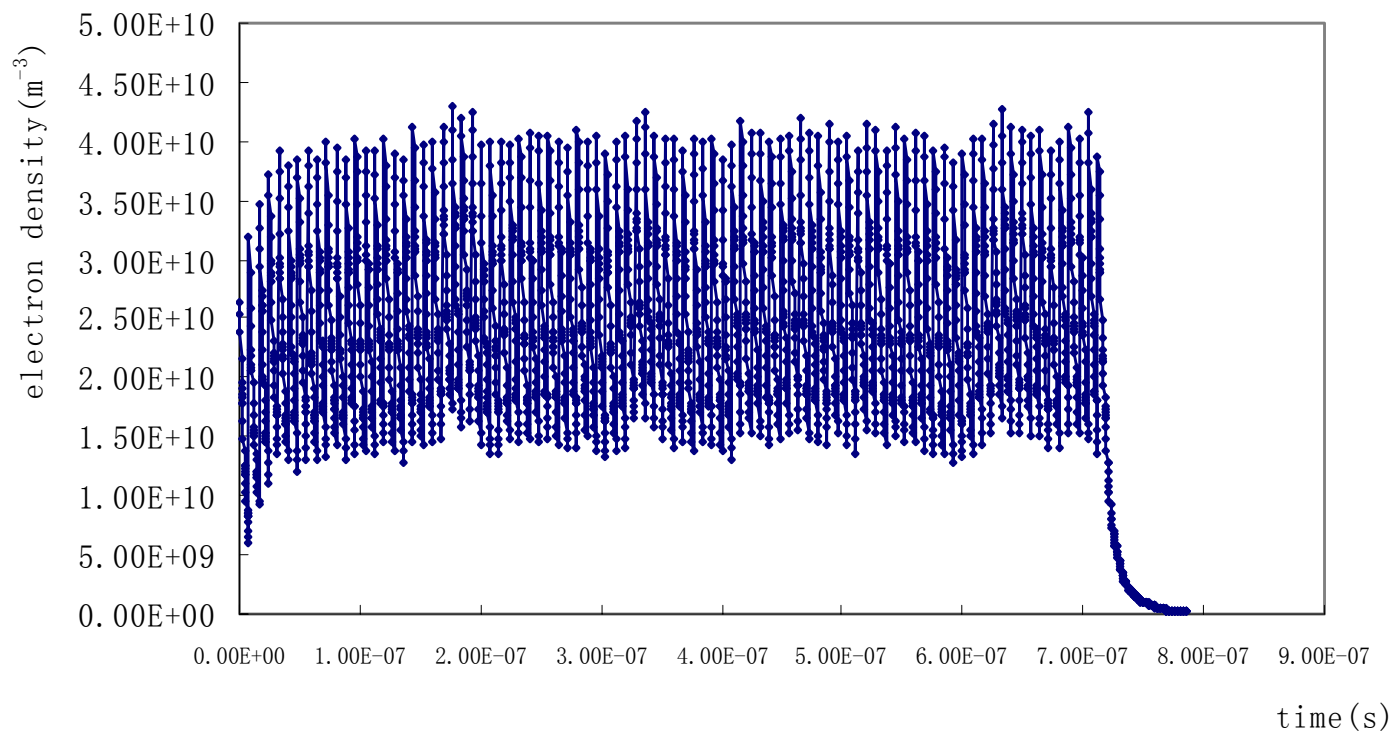


Figure 28: the average electron density of the pipe per cubic meter for a dipole magnet region with clearing electrode (1kV) vs. time.

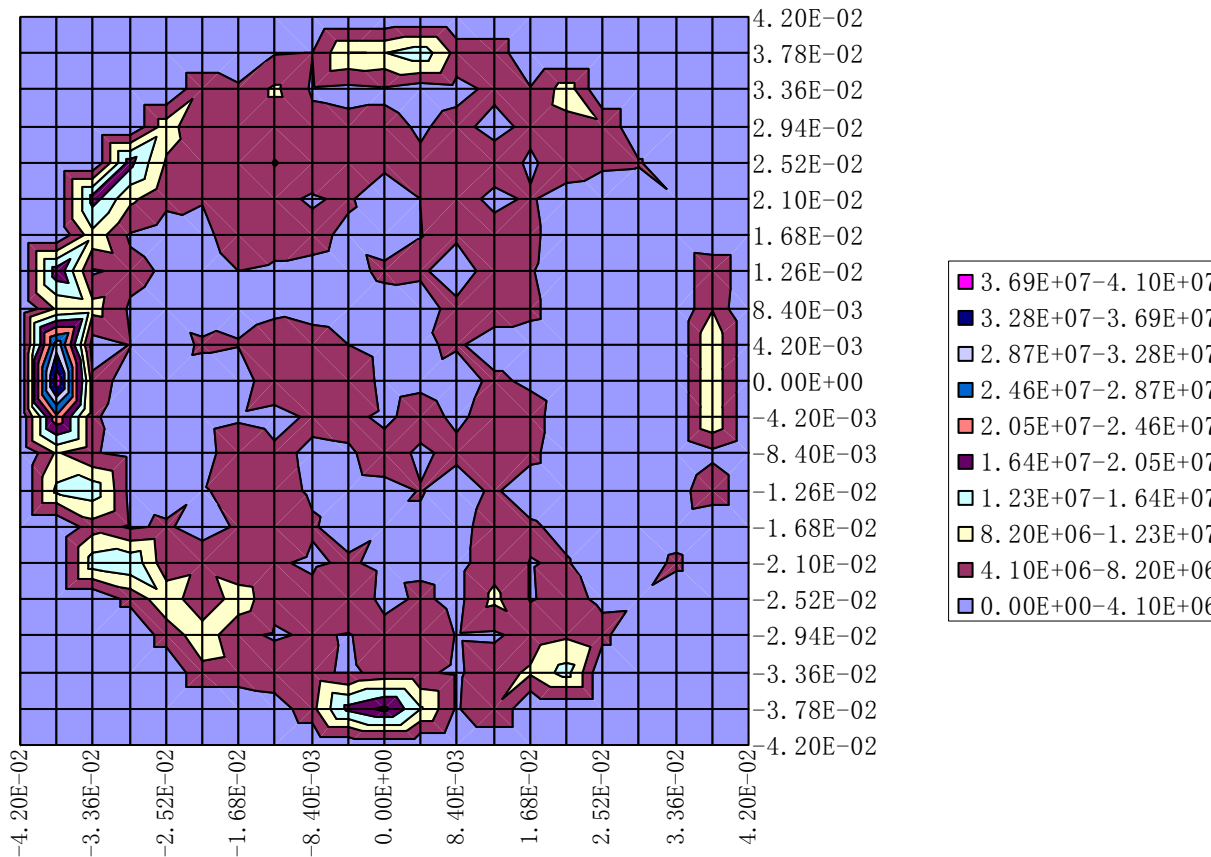


Figure 29: Transvers distribution of the electron cloud in the dipole magnet region with clearing electrode(100V) .

## 2. Instability

### coupled-bunch Instability

The “turn by turn” code developed by Dr. Y. Luo was used.

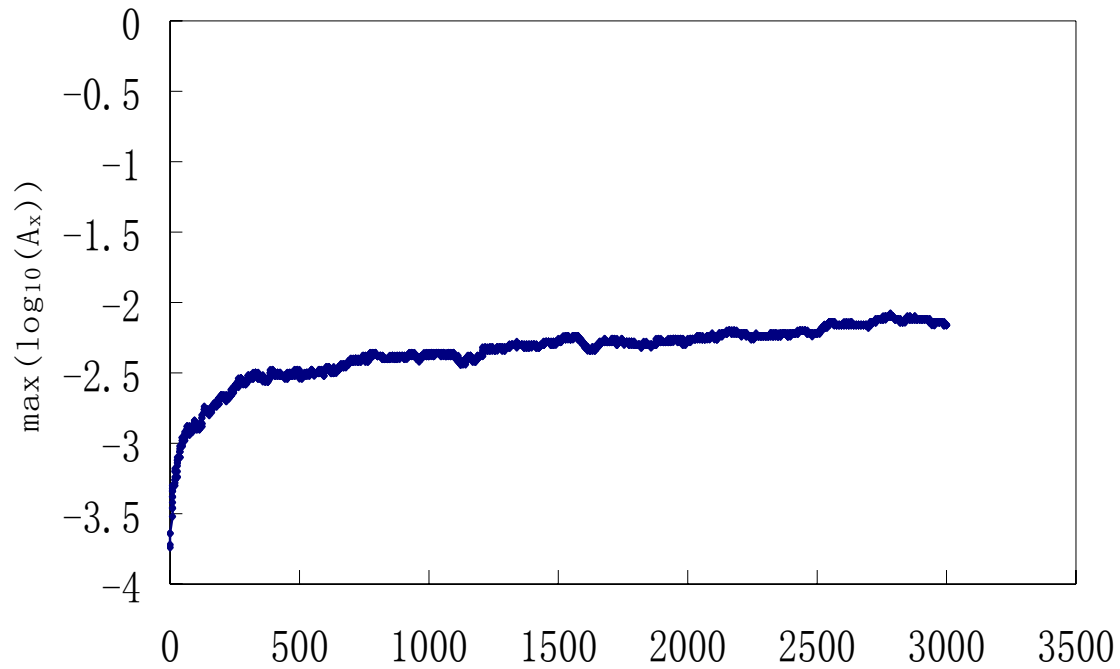


Figure.30  $\max(\log_{10}(A_x))$  vs. turns turns

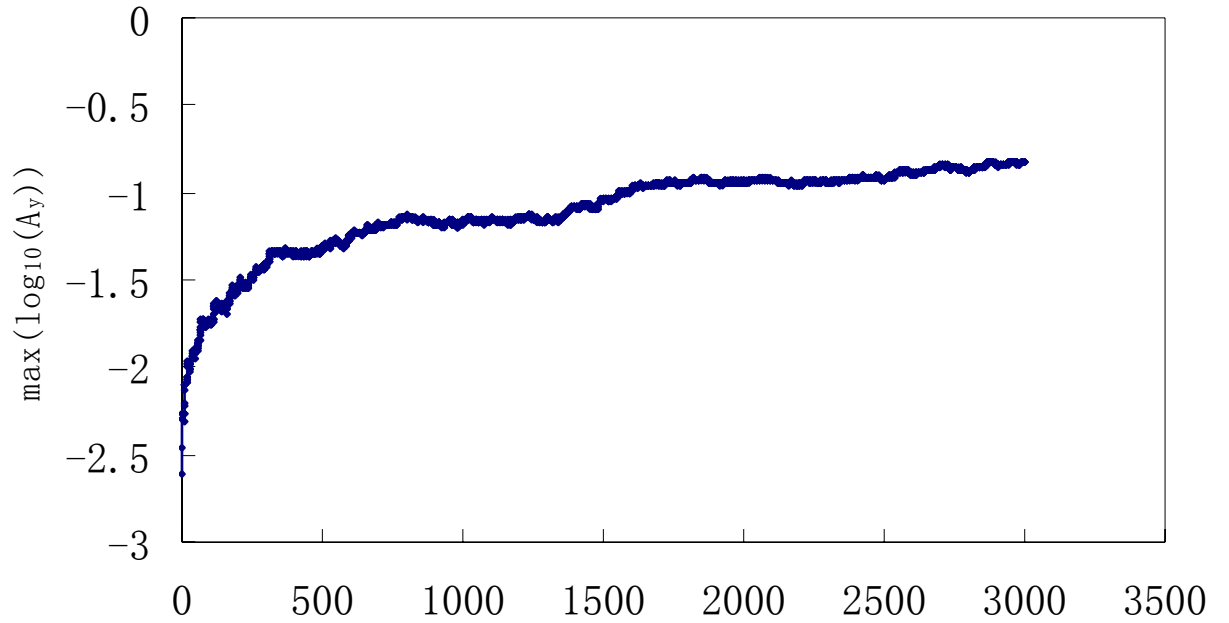


Figure. 31 max(log<sub>10</sub>(A<sub>y</sub>)) vs. turns turns

The rise time got from simulation is about 0.3ms, is agreement with that from the equation

$$\tau_{e,CB} \approx \frac{\gamma \omega_{\beta}}{2\pi r_e c^2 \rho_{el}}$$

## single-bunch Instability

The **headtail** programme developed by G. RUMOLO was used in the simulation study. Followed is part of the input file.

```
Horizontal_chromaticity: 1.0
Vertical_chromaticity: 1.0
Flag_for_synchrotron_motion: 1
Scale_factor_for_electrons_size: 4
Switch_for_wake_fields: 1
Res_frequency_of_broad_band_resonator_[GHz]: 1.6
Horizontal_quality_factor: 1.
Vertical_quality_factor: 1.
Shunt_impedance_x_[MOhm/m]: 0.066
Shunt_impedance_y_[MOhm/m]: 0.066
Flag_for_the_tune_spread_(0->no_1->space_charge_2->random): 0
Flag_for_the_e-field_calc_method_(0->no_1->soft_Gauss_2->PIC): 2
Magnetic_field_(0->no_1->dipole_field_2->solenoid): 0
x-kick_amplitude_at_t=0_[m]: 0.
y-kick_amplitude_at_t=0_[m]: 0.
Flag_for_the_proton_space_charge: 0
Flag_for_the_sc-rotation(0->local_centroid_1->bunch_centroid): 0
```

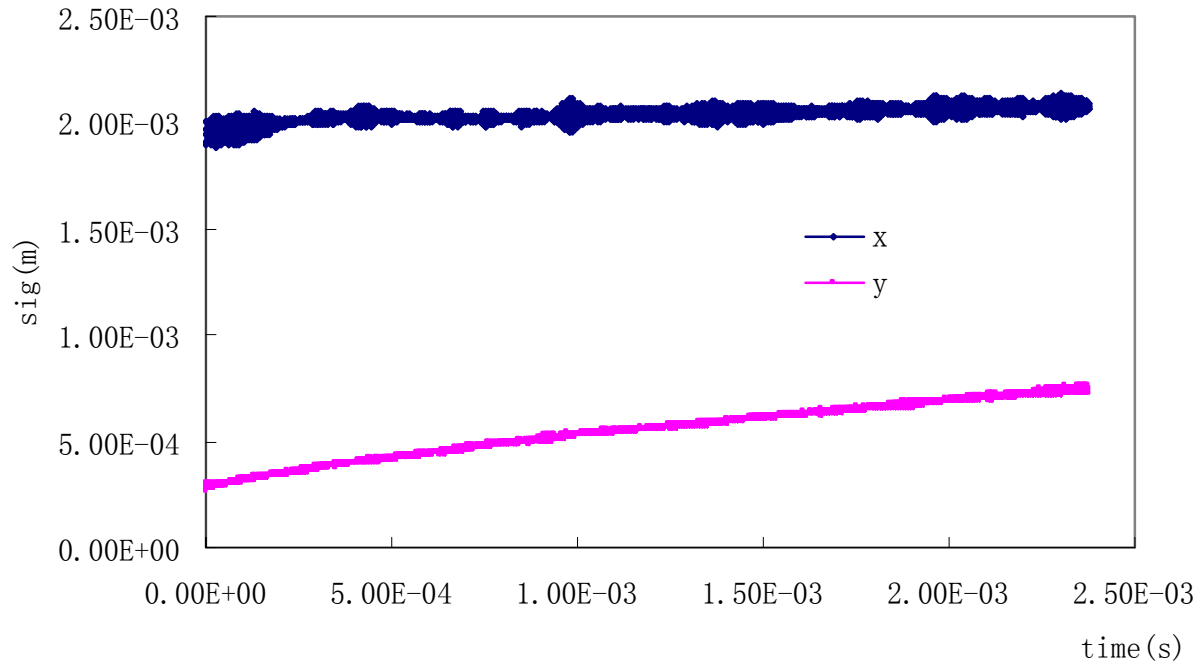


Figure32: Sqrt(beam size) growth as a function of time in the field-free region, assume the electron density is  $2.0 \times 10^{12}/\text{m}^3$ .

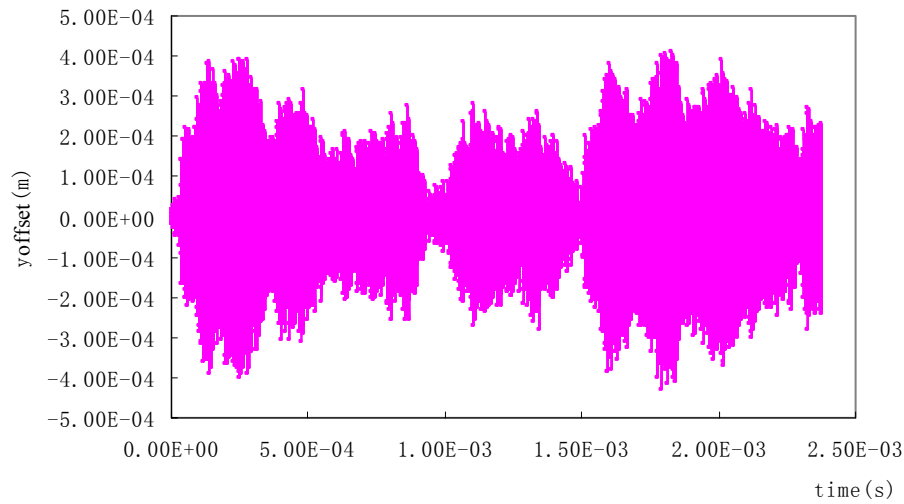
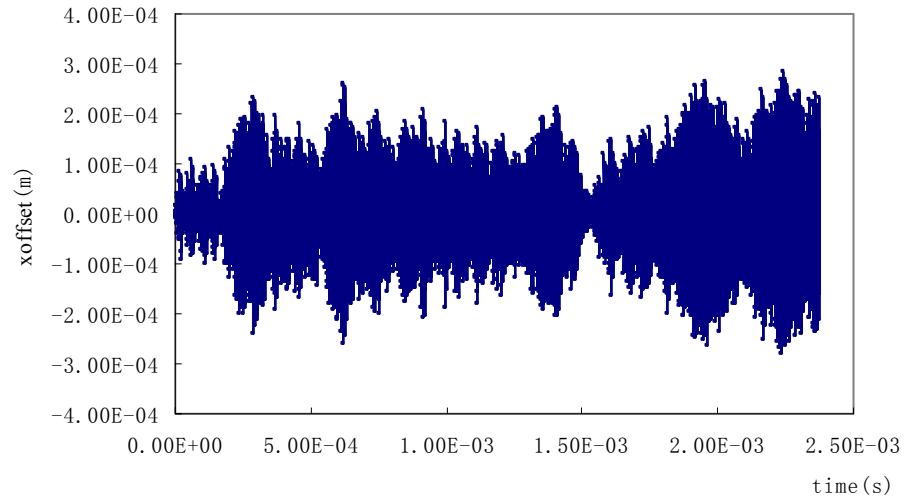


Figure 33: Simulated beam centroid motion as a function of time in the field-free region, assume the electron density is  $2.0 \times 10^{12} / \text{m}^3$ .

### **3. summary**

From the simulation result, the instabilities caused by the electron cloud seems not so seriously as expected even use the the maximum ecloud density in the field free region and think all the ring is the field free region.

One possible explanation is that the BEPCII will work under the TMCI threshold of eletron cloud volumedensity. And the other benefit is that nearly a quarter of the positron ring is the strong dipole magnet which will strongly suppress the electron cloud volume density. Also we consider the effect of the solenoid and the clearing electrode that had been successfully used to deal with the ecloud instabilities.

More study will be down on different conditions to make sure that the instabilities caused by the electron cloud will not influence the designed performance of the collider so much.